JOC The Journal of Organic Chemistry

Article

pubs.acs.org/joc

Synthesis and Electronic, Photophysical, and Electrochemical Properties of a Series of Thienylcarbazoles

Shin-ichiro Kato, Satoru Shimizu, Hiroaki Taguchi, Atsushi Kobayashi, Seiji Tobita, and Yosuke Nakamura*

Department of Chemistry and Chemical Biology, Graduate School of Engineering, Gunma University, Kiryu, Gunma 376-8515, Japan

Supporting Information

ABSTRACT: A series of thienylcarbazoles were synthesized by Suzuki–Miyaura and Ullmann coupling reactions. In these compounds, the 2-thienyl or 2,2′-bithiophen-5-yl group is connected at the *N*-, 1,8-, 3,6-, 2,7-, 2,7,*N*-, or 1,8,*N*-positions of the carbazole ring. The effects of structural variations on their electronic, photophysical, and electrochemical properties were explored by UV–vis and fluorescence spectroscopies, cyclic voltammetry (CV), and DFT calculations in evaluation of their potential as material components. The thienyl substituents at the 2,7-positions in **4**, **5**, and **10** are responsible for a high degree of π-conjugation and strong emission with fluorescence quantum yields up to 0.61. The CV on a series of thienylcarbazoles revealed a good electron-donating ability of 3,6-substituted carbazoles **3** and **9**. The number of thiophene units was found to affect the extent of π-conjugation, the resulting HOMO–LUMO gaps, and fluorescence efficiency. The crystal structures of **5** and **9** were also disclosed.

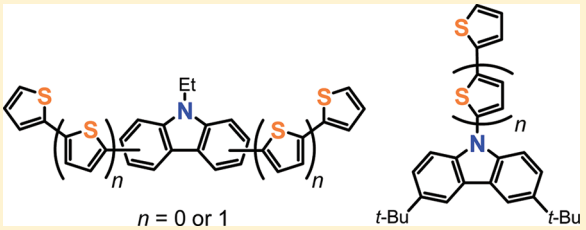

INTRODUCTION

The development of new π-conjugated organic materials is attracting growing attention due to their potential applications for various electronic and opto-electronic devices,[1] such as organic light-emitting diodes (OLEDs),[2] organic field-effect transistors (OFETs),[3] organic photovoltaics (OPVs),[4] and sensors.[5] Much effort has been devoted to establish structure–property relationships in order to develop new materials with desired properties in an intelligent way. Such systematic studies on conjugated oligomers also provide valuable insights into relevant fundamental properties of π-systems.[6]

The choice of building blocks has to be carefully examined in the molecular design of functional materials because they tend to dominate the properties in many cases. Among many heteroaromatic systems, carbazoles, their derivatives, polymers, and oligomers are a highly interesting family of functional organic molecules because carbazole has fine optical properties, a low redox potential, and high chemical stability. Oligo-/polycarbazoles[7] have been representative benchmark materials in OLEDs,[8,9] OFETs,[10] and OPVs[11] to date. Carbazole can be easily functionalized by electrophilic aromatic substitution at its 3,6-positions (*para* position from the nitrogen atom) with high electron density, and hence a large number of 3,6-functionalized carbazole derivatives have been studied. The 1,8-functionalized carbazoles can be obtained when the 3,6-positions of carbazole are first protected, because its 1,8-positions (*ortho* position from the nitrogen atom) are also activated.[12−14] Although the synthesis of 2,7-functionalized carbazoles is not straightforward, the efficient synthetic pathways to them have been established in the past decade, and their applications to various functional devices have been extensively investigated by Leclerc and co-workers.[7b−d] In any of these cases, the nitrogen atom of the carbazole moiety can be also functionalized by alkylation or arylation reaction to enhance the solubility and other properties of the resulting carbazole derivatives. Thus, carbazole would be recognized as a useful scaffold to allow the large structural diversity for fine-tuning of optical and electrochemical properties.

Thiophene derivatives, in particular oligothiophens, are now excellent candidates for a variety of advanced materials applications.[15] Therefore, mixed π-conjugated polymers and oligomers made of carbazoles and thiophenes are a new class of functional compounds through the use of their highly electron-donating ability. For example, Jen and co-workers reported the high performance of poly(3,6-carbazole)s incorporating diethynylthiophene units in OLED.[16] Zotti, Leclerc, and co-workers synthesized poly(2,7-carbazole)s incorporating thiophene units, and their conductive properties were investigated.[17] More recently, Melucci and co-workers synthesized 3,6-bis(2,2′-bithiophen-5-yl)-9-methyl-9*H*-carbazole derivatives with suitable alkyl chains as liquid-crystalline semiconducting materials.[18] Some oligomers consisting of carbazole and thiophene units were also synthesized;[19,20] however, no systematic study on structurally well-defined carbazole–thiophene systems focusing on the effect of the conjugation connectivity between the carbazole and thiophene units on their electronic, optical, and electrochemical properties has been reported so far, to the best of our knowledge. In this context, we became interested in thienyl-substituted carbazole derivatives, namely, thienylcarba-

Received: December 23, 2011
Published: February 28, 2012

   dx.doi.org/10.1021/jo202625p | J. Org. Chem. 2012, 77, 3222–3232

Chart 1

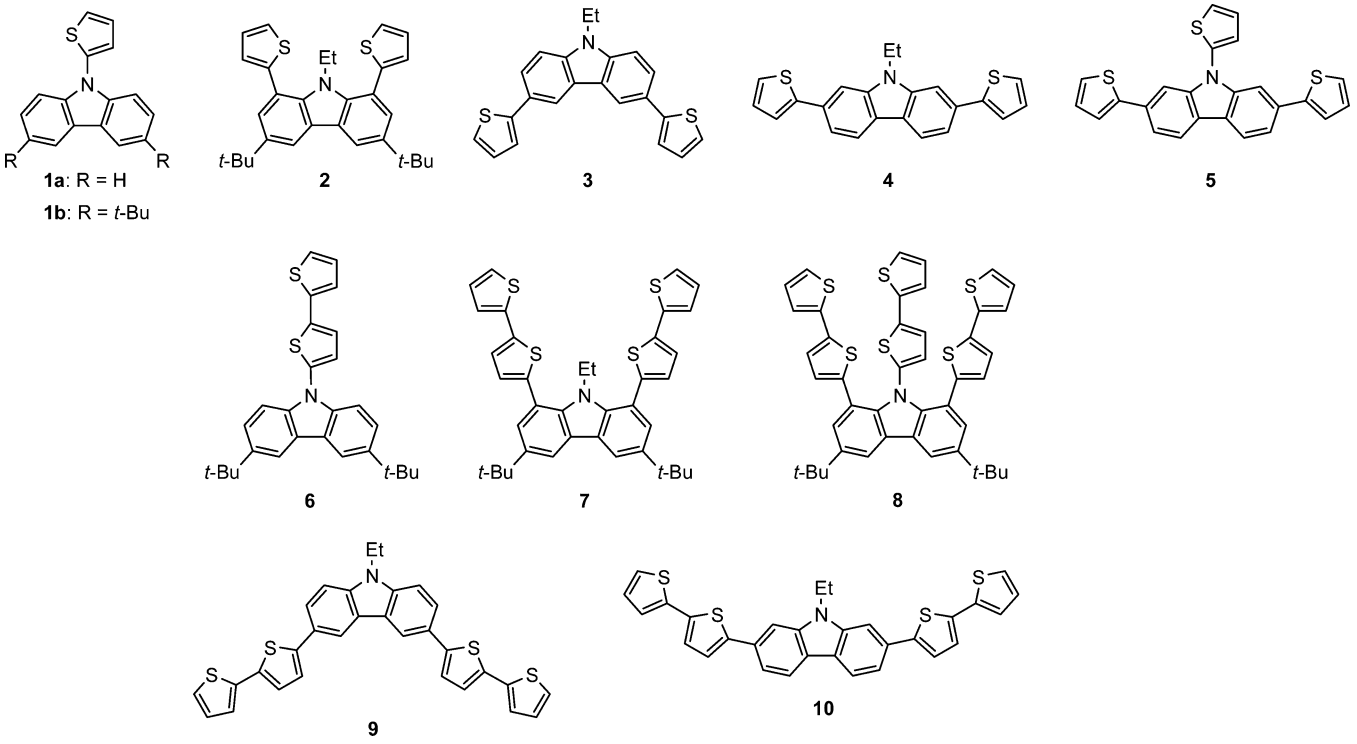

zoles **1**–**10**, in which a thienyl group is incorporated into a carbazole moiety at the *N*-, 1,8-, 3,6-, 2,7-, 2,7,*N*-, and 1,8,*N*-positions (Chart 1). A large series of thienylcarbazoles **1**–**10** varying the conjugation connectivity and the number of thiophene units allow us to study the structure–property relationships of carbazole–thiophene-based materials. Here, we report the synthesis and fundamental properties, such as the structural features and the electronic, photophysical, and redox properties, of **1**–**10** on the basis of X-ray crystallographic study, UV–vis and fluorescence spectroscopies, cyclic voltammetry, and theoretical calculations.[21]

RESULTS AND DISCUSSION

Synthesis. In our molecular design, the 2-thienyl or 2,2′-bithiophen-5-yl group was incorporated into the carobazole moiety. To functionalize the 1,8-positions of carbazole, *tert*-butyl groups were first introduced to the 3,6-positions in **2**, **7**, and **8** by Friedel–Crafts reactions with 2-chloro-2-methylpropane.

Compounds **1a**,[22] **1b**,[23] and **3**[24] are known in the literature. Thienylcarobazoles **2** and **4**–**10** were synthesized via Suzuki–Miyaura cross-coupling[25] and/or Ullmann coupling reactions[26] as key steps (Schemes 1–4). For Suzuki–Miyaura cross-coupling, $Pd(PPh_3)_4$ as a catalyst was used and 1,8-disubstituted carbazole **2** was obtained from 1,8-dibromocarbazole derivative **11** and 2-thiopheneboronic acid pinacol ester (**12**) in 32% yield (Scheme 1). Similar cross-coupling reactions were performed on 2,7-dibromocarbazole derivative **13** with either **12** or 2,2′-bithiophene-5-boronic acid pinacol ester (**14**) to give thienylcarbazoles **4** and **10** in 68% and 81%, respectively (Scheme 2). Compound **5** was obtained from 2,7-dibromocarbazole (**15**) in two steps. The Ullmann coupling reaction of **15** with 2-bromothiophene in the presence of copper powder and K_2CO_3 in nitrobenzene afforded dibromide **16** in 75% yield. The Suzuki–Miyaura cross-coupling reaction was then

Scheme 1. Synthesis of 2

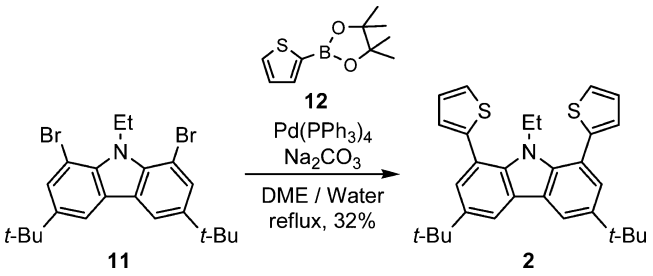

performed on **16** and **12** to give **5** in 92% yield. The Ullmann coupling reaction of 3,6-di-*tert*-butylcarbazole (**17**) with bromide **18** afforded **6** in 20% yield (Scheme 3). Thienylcarbazole **7** was synthesized following a two-step transformation from diiodocarbazole derivative **19**. The ethylation of **19** with iodoethane was carried out in the presence of NaOH as a base in DMF, and then the cross-coupling reaction of **20** with **14** afforded the desired **7**. The synthesis of **8** was achieved by sequential coupling reactions. Thus, **8** was prepared from **19** by the Suzuki–Miyaura coupling with **14** followed by the Ullmann coupling with **18**. The Suzuki–Miyaura coupling reaction of dibromocarbazole derivative **22** with **14** gave **9** in 85% yield (Scheme 4). All compounds were fully characterized by various spectroscopic methods, such as ^{1}H NMR, ^{13}C NMR, and mass spectroscopy.

Structural Properties. The single crystals of **5** and **9** suitable for X-ray crystallographic analyses were successfully obtained by slow diffusion of hexane into $CHCl_3$ at 0 °C (Figure 1a,b).[27] The structure determined for **5** exhibited the statistical disorder of the two thiophene rings at the 2,7-positions (Supplementary Figure S1 in the Supporting Information). In **5**, the 2,7-di(2-thienyl) and carbazole moieties are quasi-coplanar with dihedral angles for C9–C10–C24–

dx.doi.org/10.1021/jo202625p | J. Org. Chem. 2012, 77, 3222–3232

Scheme 2. Synthesis of 4, 5, and 10

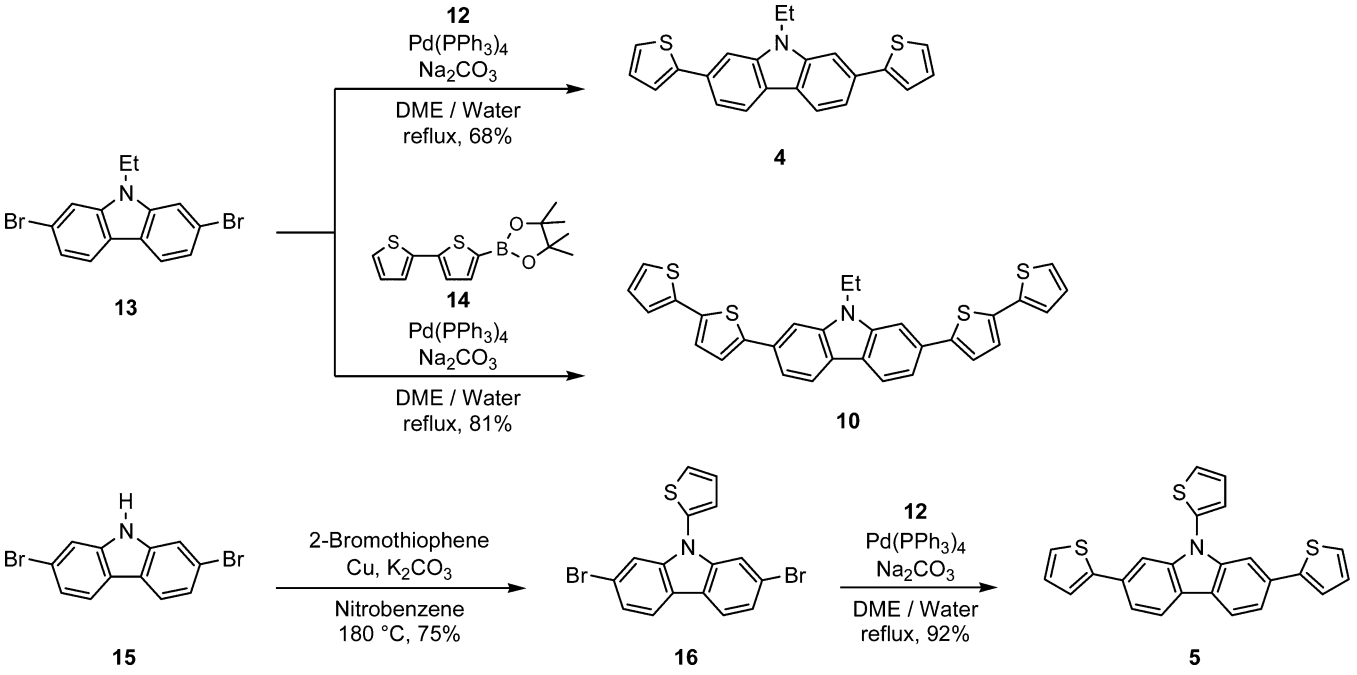

Scheme 3. Synthesis of 6–8

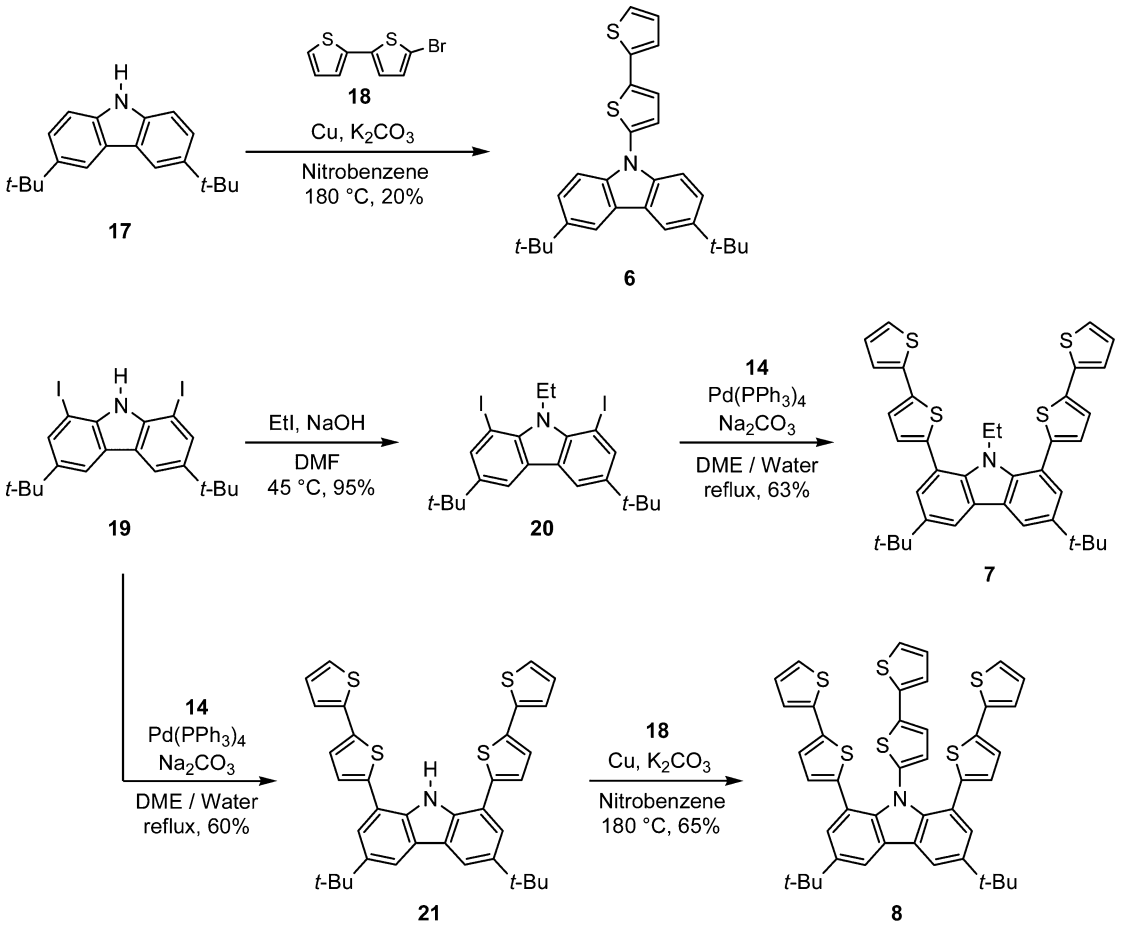

C23 and C2–C3–C17–C20 of 170.1° and 14.9°, respectively (Figure 1a). The *N*-(2-thienyl) and carbazole moieties are nearly orthogonal with a dihedral angle for C14–C13–N1–C1 of −107.9°. This is apparently ascribed to steric repulsions between the 1,8-hydrogen atoms in the carbazole moiety and the attached *N*-(2-thienyl) moiety. Thienylcarbazole **9** also exhibited the disorder of the peripheral thiophene rings in the solid state. There are three crystallographically independent

dx.doi.org/10.1021/jo202625p | *J. Org. Chem.* 2012, 77, 3222–3232

Scheme 4. Synthesis of 9

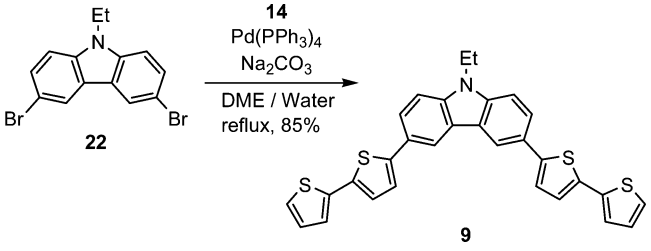

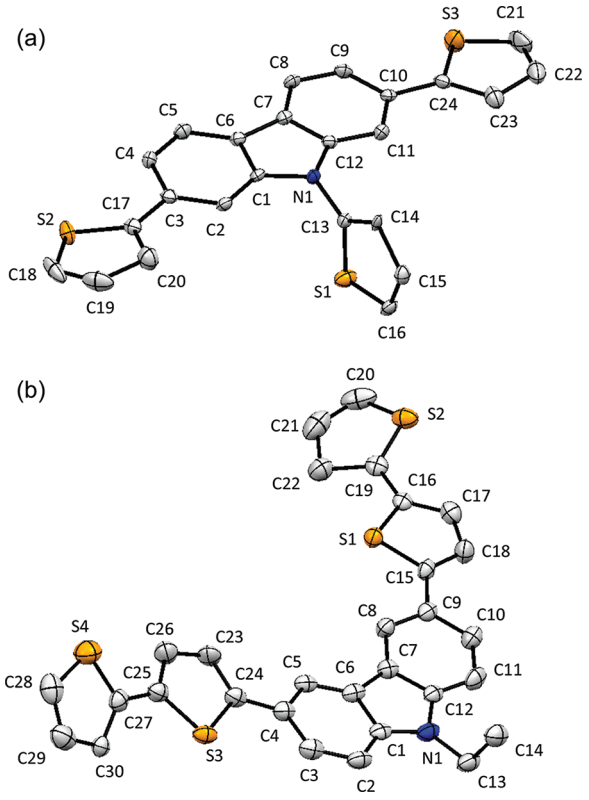

Figure 1. ORTEP plots of (a) **5** and (b) **9** with displacement ellipsoids at 50% probability level at 153 K. Arbitrary numbering; hydrogen atoms are omitted for clarity. One of the three different molecules in the unit cell is shown for **9**.

molecules for **9** in the unit cell. The largest difference among them is the conformation between the thiophene rings and the carbazole π-system. The two molecules adopt the two-*s*-*cis* conformations, while the *s*-*cis* and *s*-*trans* conformations coexist in the one molecule (Figure 1b and Supplementary Figure S2). The torsional angles between the carbazole π-system and the attached 3,6-bis(2,2′-bithiophen-5-yl) moiety vary from 0.6° to 33.9°. In the density functional theory (DFT)-optimized structure of **9** at the B3LYP/6-31G* level of theory without any symmetry constrains by the Gaussian 03 suit of program,[28] the torsional angle is estimated to be approximately 25°. Therefore, it is likely that the observed deviation of the torsional angles from the calculated one is derived from the crystal packing force. The bithiophene systems in the solid-state structure of **9** are nearly planar with a torsional angle of approximately 16° as a mean value. Pyramidalization of the nitrogen atoms is insignificant in both **5** and **9**. This is expressed by the sums of the three bond angles at these nitrogen atoms of 354.8° and 359.6° in **5** and **9**, respectively. The selected geometrical parameters of **5** and **9** obtained by the DFT calculations are given in Supplementary Tables S1 and S2, respectively, and compared with the crystallographic bond lengths and torsion angles. In general, there is good agreement between the experiment and theory. The differences in carbon−carbon bond lengths in the carbazole moieties are within 0.02 Å. The large deviation occurs for the above-mentioned torsional angles between the carbazole π-system and the thienyl units and the carbon−sulfur bond lengths in the thiophene moieties. Thus, the DFT results provide slightly longer bond lengths by 0.023−0.039 Å compared with the X-ray results.

Electronic Absorption Spectroscopy. The UV−vis absorption spectral data of **1**−**10** in CH_2Cl_2 are summarized in Table 1. Notably, the extent of π-conjugation is highly dependent on the substituent pattern of the carbazole moiety and the number of thiophene units.

The absorption spectra of **1a** and **2**−**5** having the 2-thienyl functionality are shown in Figure 2a. Thienylcarbazole **1a** features the longest absorption maximum (λ_{max}) of 333 nm with a molar extinction coefficient (ε) of 4000 M^{-1} cm^{-1}, while **1b** displays the bathochromically shifted longest λ_{max} of 340 nm with ε of 3900 M^{-1} cm^{-1} (Figure 2b). The absorption curves of **1a** and **1b** are similar to those of *N*-ethylcarbazole (**23**) and 3,6-

Table 1. Optical Data and Calculated Lowest Excitation Energies of 1−10

	λ_{max} [nm][a]	λ_{onset} [nm][b]	λ_{em} [nm][a]	Φ_{em}[c]	calcd λ_{max} [nm][d] (f)	composition of band[d]
1a	285,[e] 291, 322, 333	345	370	0.014	307 (0.015)	H → L, 33%; H → L + 1, 60%
1b	285,[e] 295, 329, 340	355	368	*f*	313 (0.038)	H → L, 23%; H → L + 1, 69%
2	290, 305,[e] 345, 360[e]	380	395	0.064	335 (0.074)	H−1 → L + 3, 3%; H → L, 88%
3	256, 267, 314, 345[e]	385	392, 411	0.047	329 (0.330)	H−1 → L + 1, 9%; H → L + 1, 81%
4	269, 290,[e] 353, 370[e]	395	391, 412	0.610	352 (1.128)	H → L, 84%
5	261, 292, 352	390	387, 407	0.210	352 (1.179)	H → L, 84%
6	260,[e] 285,[e] 296, 325,[e] 340	390	417	0.129	375 (0.216)	H−2 → L, 4%; H → L, 89%
7	310, 325,[e] 360[e]	415	440	0.106	374 (0.274)	H−2 → L, 9%; H → L, 89%
8	305, 340[e]	390	434	0.092	372 (0.013)	H → L, 76%; H → L + 1, 14%; H → L + 2, 3%
9	353, 380[e]	430	430, 450[e]	0.168	395 (1.146)	H → L, 87%
10	256, 313, 399	455	447, 472	0.482	421 (1.964)	H → L, 87%

[a]In CH_2Cl_2. [b]The longest energy absorption wavelength with a molar absorptivity ε = 500 M^{-1} cm^{-1}. [c]Absolute quantum yields determined by a calibrated integrating sphere system in cyclohexane. [d]TD-DFT (TD/B3LYP/6-31G*) calculations were carried out with the use of optimized structures at B3LYP/6-31G* level of theory, and only energies with f > 0.01 are shown; f = oscillator strength; H = HOMO, L = LUMO. [e]Peak as shoulder. [f]Not measured.

dx.doi.org/10.1021/jo202625p | J. Org. Chem. 2012, 77, 3222−3232

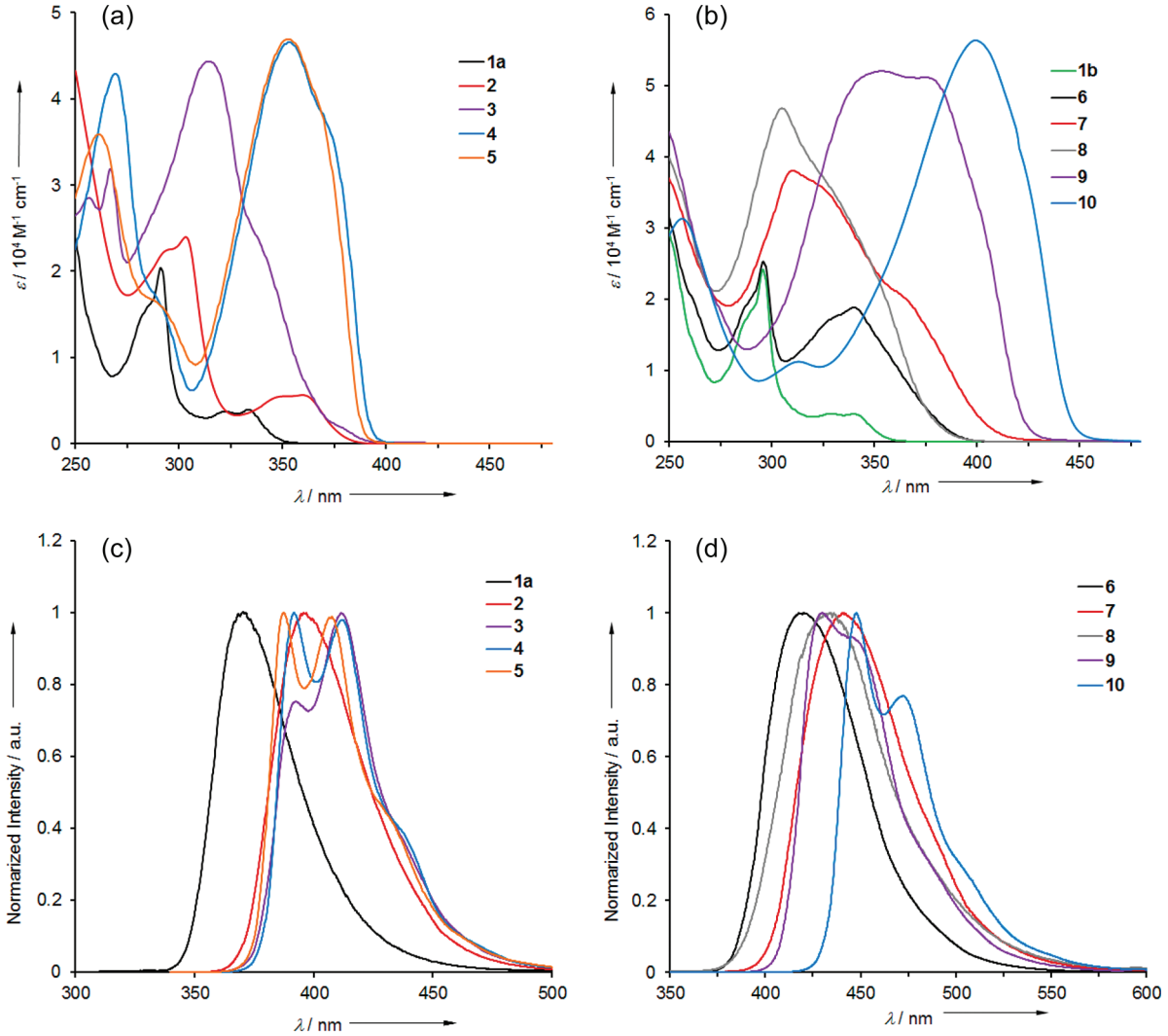

Figure 2. Electronic absorption spectra of (a) **1a** and **2**–**5** and (b) **1b** and **6**–**10** and normalized fluorescence spectra of (c) **1a** and **2**–**5** and (d) **6**–**10** in CH_2Cl_2.

di-*tert*-butyl-*N*-ethylcarbazole (**24**), respectively. The longest λ_{max} values of **1a** and **1b** are hypochromically shifted relative to those of **23** and **24**, respectively: **23**, 346 nm, **24**, 353 nm (Supplementary Figure S4). These results show almost no π-conjugation between the carbazole and thiophene moieties, which should reflect steric hindrance between the *N*-(2-thienyl) moiety and the 1,8-hydrogen atoms in the carbazole moiety as expected from the crystal structure of **5**. The longest λ_{max} of 1,8-disubstituted carbazole derivative **2** is bathochromically shifted relative to that of **24** by only approximately 5 nm, indicative of less effective conjugation between the carbazole and thiophene moieties in **2** probably due to the twist around the C–C bonds connecting them. Compound **3** displays a different absorption curve from those of **1a,b** and **2** along with the significantly increased absorptivity in the whole region. When compared to **3**, **4** features the significantly bathochromic shift of the longest λ_{max} of 353 nm with higher ε of 46400 M^{-1} cm^{-1}. Interestingly, **5** displays almost the same absorption curve as that of **4** in a region of 320–400 nm, featuring the absorption maximum of 352 nm with ε of 46900. Thus, the electronic property of **5** in the ground state is mainly dominated by the 2,7-di(2-thienyl) substitution, which is further confirmed by theoretical calculations described below.

The UV–vis spectra of **6**–**10** having the 2,2′-bithiophen-5-yl functionality are shown in Figure 2b. The 2,2′-bithiophen-5-yl substitutions in **6**, **7**, **9**, and **10** intrinsically resulted in the extension of π-conjugation, that is, the reduction of HOMO–LUMO gaps relative to those of the corresponding **1b**, **2**, **3**, and **4**. For example, the extension of the chromophore in nearly planar **9** readily gives rise to the spectral change as compared to **3**. Thus, the spectrum of **9** is highly broadened, and its absorption onset (λ_{onset}) as well as the longest λ_{max} are bathochromically shifted, clearly reflecting the effective π-conjugation as expected by its X-ray crystal structure. Similarly, the longest λ_{max} of **10** is bathochromically shifted relative to that of **4** by approximately 30 nm, and hence **10** has the smallest optical HOMO–LUMO gap in the series of **1**–**10** (Table 1). The similar effect of the number of thiophene units on the extension of conjugation is also seen in nonplanar **6**–**8**. Compound **6** features the longest λ_{max} of 340 nm with ε of 18900 M^{-1} cm^{-1}, and its λ_{onset} (390 nm) is bathochromically shifted by approximately 35 nm as compared with that of **1b** (355 nm). The spectrum of **6** is apparently different from the superposition of the spectra of **24** and 2,2′-bithiophene (**25**), which shows the effective π-conjugation between the 2,2′-bithiophen-5-yl group and the carbazole backbone in **6**

dx.doi.org/10.1021/jo202625p | J. Org. Chem. 2012, 77, 3222–3232

(Supplementary Figure S5). The DFT calculations at the B3LYP/6-31G* level of theory predict that there is no significant difference of the dihedral angles between the carbazole and thiophene moieties in **1b** and **6**: 69° in **1b** and 66° in **6** (Figure 3).[29] The longest λ_{max} for **7** appears at 360 nm as a shoulder, which is almost consistent with that of **2**; however, the λ_{onset} of **7** (415 nm) is red-shifted relative to that

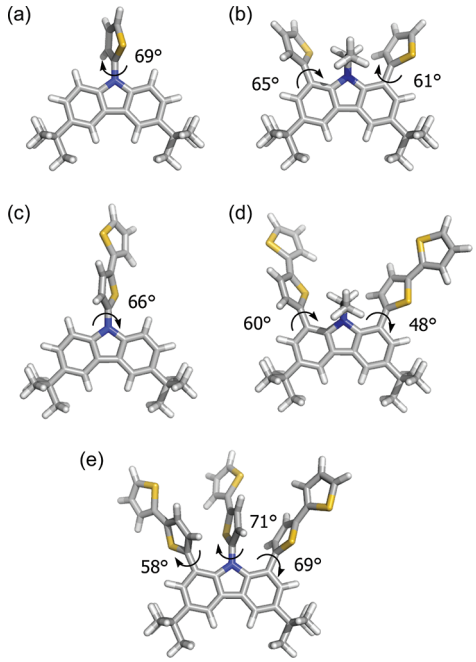

Figure 3. Optimized structures of (a) **1b**, (b) **2**, (c) **6**, (d) **7**, and (e) **8** at the B3LYP/6-31G* level of theory.

of **2** (380 nm). On the basis of the calculations, the twist around the C−C single bonds connecting the carbazole moiety to the thienyl moieties in **7** is expected to be smaller than that in **2**: 61° and 65° in **2** and 48° and 60° in **7**. This may be one of the reasons for the extension of π-conjugation of **7** relative to **2**. However, we do not have a suitable explanation for the π-conjugative effect in **6** as compared to **1b** at present. Further introduction of the 2,2′-bithiophen-5-yl group on the nitrogen atom in **8** leads to a hypochromic shift of the longest λ_{max} as well as the absorption onset as compared to **7**, although the ε value around 300 nm of **8** is slightly increased. The sterically crowded 2,2′-bithiophen-5-yl groups in **8** induce the significant twist around the C−C and/or N−C single bonds connecting the carbazole π-system to the 2,2′-bithiophen-5-yl group, which should result in the less effective π-conjugation in **8** as compared to **7**. Indeed, the DFT calculations predict that the dihedral angles between the carbazole and the 2,2′-bithiophen-5-yl moieties increase from 48° and 60° in **7** to 58° and 69° in **8**, and the *N*-(2,2′-bithiophen-5-yl) moiety in **8** is twisted from the central carbazole moiety by 71° (Figure 3).

Importantly, the effect of the thienyl functionalization at the different positions of the carbazole moiety on the extent of π-conjugation is clearly observable in the UV−vis spectral data of **6**−**10**, because they differ much in both the longest λ_{max} values and the absorption onset. Thus, thienylcarbazole systems follow the established trend of the substitution pattern for the extent of π-conjugation: *N*-, 1,8- < 3,6- < 2,7-substitution. Similar effect of the substitution pattern of the carbazole moiety on the extent of π-conjugation is found in our recent bicarbazole systems[30] as well as in others.[7b,c,8g]

Fluorescence Spectroscopy. All compounds in this study are fluorescent. The fluorescence spectra for **1a**−**5** and **6**−**10** in CH_2Cl_2 are shown in Figure 2c and d, respectively. The data are also summarized in Table 1. The fluorescence spectra were recorded in the dilute regime (10^{-5}−10^{-6} M). No characteristic excimer fluorescence was observed.[31] The color of the fluorescence of **1**−**5** and **6**−**10** ranges from violet to light blue and from blue to light green, respectively. Similar to the change of the longest λ_{max} values of **1**−**10** as described above, the emission maxima (λ_{em}) of **6**−**10** are bathochromically shifted compared to those of the corresponding **1**−**5**, depending on the number of thiophene units. The substitution pattern of the carbazole moiety also has a substantial effect on the fluorescence wavelength. For instance, 3,6-functionalized carbazole derivative **9** exhibits emission with λ_{em} values of 430 and 450 nm, while 2,7-functionalized carbazole **10** features λ_{em} values of 447 and 472 nm, which is the longest among the compounds in this study. The two well-defined vibronic maxima were observed in **3**−**5**, **9**, and **10**, while a single maximum appeared in **1a,b**, **2**, and **6**−**8**. This finding indicates a somewhat large structural change and/or electronic distribution change between the ground and excited states for **1a,b**, **2**, and **6**−**8**. The electronic absorption spectra of **4**, **5**, and **10** do not seem to be mirror images of fluorescence spectra. The longest absorption bands of the 2,7-functionalized carbazoles **4**, **5**, and **10** are probably ascribed to two different transitions, which may reflect the two well-resolved peaks in their fluorescence spectra. We note a shoulder around 370 nm in the absorption spectra of **4** in addition to the strong absorption peak at 353 nm.

The fluorescence quantum yields (Φ_{em}) of **1**−**10**, which were determined by a calibrated integrating system, vary from 0.014 to 0.610 (Table 1). In a series of **1**−**5**, the Φ_{em} values were dramatically affected by the substitution pattern. The lowest Φ_{em} value was observed in **1a** to be 0.014, which is almost 1/30th of that (*ca.* 0.4) of **23**.[32] Both **2** and **3** also display smaller Φ_{em} values than **23** by about 1 order of magnitude. In sharp contrast to **2** and **3**, compound **4** displays the significantly high Φ_{em} of 0.610, which is the highest value in a series of **1**−**10** in the present study and also higher than that of **23**. The Φ_{em} value (0.210) of **5** is almost one-third that of **4**, which should be attributed to the *N*-(2-thienyl) group in **5**. The 2,2′-bithiophen-5-yl substitution essentially brings about higher Φ_{em} values than the 2-thienyl substitution as found in **6**−**9**. The Φ_{em} values of **7** and **9** are almost 2−2.5 times as high as those of **2** and **3**, respectively, while **10** displays the slightly low Φ_{em} value (0.482) relative to that of **4**. Thienylcarbazoles **4** and **10** are remarkably emissive, which clearly confirms that the thienyl substitution at the 2- and/or 7-positions of the carbazole moiety is crucial to ensure high Φ_{em} values,[33,34] although the reason for this finding is unclear at present. Lee and co-workers reported that 4,4′-di(2-thienyl)biphenyl shows a remarkably high fluorescence quantum yield of 0.79.[35] Compounds **4** and **10** can be regarded as the nitrogen-bridged analogues. The aforementioned high Φ_{em} values of **4** and **10** may be attributed to the structural similarity between the 2,7-functionalized carbazoles and 4,4′-di(2-thienyl)biphenyl.

Electrochemistry. To investigate the effect of the thienyl functionalization of the carbazole moiety on the electron-donating ability, that is, the HOMO level, we carried out the cyclic voltammetry (CV) for **1**−**10** as well as **23** and **24** in

dx.doi.org/10.1021/jo202625p | *J. Org. Chem.* 2012, 77, 3222−3232

CH_2Cl_2 with *n*-Bu_4NPF_6 (0.1 M) as the supporting electrolyte. The oxidation potentials (E_{pa}) versus Fc^+/Fc (ferrocenium/ferrocene couple) are listed in Table 2. Thienylcarbazoles **1**–**10** displayed a carbazole-type 1 e^- oxidation step, which was irreversible except for **2**, between +0.47 and +0.88 V. The oxidation peak amplitude in the CV was quite large after the first oxidation, which should be attributed to the accumulation of the compounds at the electrode surface by electrochemical polymerization.

Table 2. Oxidation Potential (E_{pa}) by Cyclic Voltammetry in CH_2Cl_2 (0.1 M *n*-Bu_4NPF_6),[a] Theoretically Calculated HOMO and LUMO Levels,[b] and Optical HOMO–LUMO Gaps (ΔE_{opt})[c]

	E_{pa} [V][d]	HOMO [eV]	LUMO [eV]	$\Delta E_{HOMO-LUMO}$ [eV]	ΔE_{opt} [eV]
1a	+0.88	−5.74	−1.05	4.69	3.59
1b	+0.73	−5.54	−0.97	4.57	3.49
2	+0.75	−5.47	−1.26	4.21	3.26
3	+0.54	−5.31	−1.21	4.09	3.22
4	+0.65	−5.44	−1.66	3.78	3.13
5	+0.74	−5.47	−1.70	3.77	3.17
6	+0.60	−5.47	−1.68	3.79	3.17
7	+0.64	−5.36	−1.67	3.69	2.98
8	+0.68	−5.41	−1.60	3.81	3.17
9	+0.47	−5.14	−1.67	3.47	2.88
10	+0.50	−5.21	−1.98	3.22	2.72
23	+0.89	−5.55	−0.96	4.58	3.49
24	+0.71	−5.37	−0.89	4.48	3.39

[a]All potentials are given versus the Fc^+/Fc couple used as external standard; scan rate = 0.1 V s^{-1}. [b]B3LYP/6-311G**//B3LYP/6-31G*. [c]The values are obtained from λ_{onset}. [d]No reversible peak was observed except for **2** and **24**.

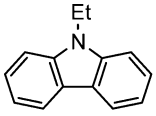

23

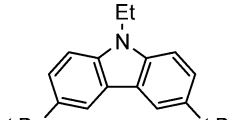

24

Thienylcarbazoles **1a** and **1b** showed oxidation peaks at +0.88 and +0.73 V, respectively, which are almost comparable to those of **23** and **24**, respectively. This clearly demonstrates that there is almost no effective π-conjugation between the carbazole and thiophene moieties in **1a,b** by the steric effects as discussed above, and thereby, their *N*-(2-thienyl) groups do not contribute to the donor potency. Again, the 1,8-di(2-thienyl) groups in **2** have almost no influence on the electron-donating ability, and thus **2** is oxidized at +0.75 V. On the contrary, **3** and **4** are oxidized cathodically relative to **23** by 350 and 240 mV, respectively. The value of +0.54 V in **3** is the lowest in a series of **1**–**5**. Compound **4** exhibits an anodic shift of the E_{pa} value by 110 mV as compared to **3**, which is readily explained by the substitution pattern of the carbazole moiety. The 3,6-di(2-thienyl) substituents of **3** are located at the *para* positions relative to the nitrogen atom of the carbazole moiety, while the 2,7-di(2-thienyl) substituents of **4** are at the *meta* positions. Hence, the electron-donating ability of the carbazole moiety in **3** is enhanced by the 3,6-di(2-thienyl) groups, while the enhancement of that in **4** is insufficient due to the cross-conjugation. The presence of the additional *N*-(2-thienyl) group in **5** brings about an anodic shift of its oxidation potential relative to **4** by 90 mV. This implies that the σ-inductive effect by the *N*-(2-thienyl) group in **5**, which is nearly orthogonal to the carbazole backbone as confirmed by the X-ray analysis, lowers the HOMO level relative to that of **4**.

Upon increasing the number of thiophene units from **1b**, **2**, **3**, and **4** to **6**, **7**, **9**, and **10**, respectively, the oxidations occur at potentials cathodically shifted by 90–150 mV.[36] Compound **6** exhibits a substantial cathodic shift of the E_{pa} value by 130 mV as compared to the corresponding **1b** with the *N*-(2-thienyl) group. Similarly, **7** is oxidized more cathodically than **2** by 110 mV. The efficient π-conjugation in **6** and **7** relative to **1b** and **2**, respectively, as observed in the electronic absorption spectra should make their oxidation potentials cathodic. Interestingly, the E_{pa} value (+0.68 V) of **8** is less negative as compared to those of **6** and **7**, despite the presence of the three 2,2′-bithiophene units. It is clear that the somewhat high E_{pa} value of **8** is a consequence of the less effective π-conjugation between the 2,2′-bithiophen-5-yl and carbazole moieties by the steric effects. From **3** to **9**, the cathodic shift is observed to be 70 mV, and thus the oxidation of **9** occurs at +0.47 V, which is the lowest in a series of compounds in this study. The oxidation potential of **10** shifts cathodically by 150 mV relative to that of **4** upon 2,7-bis(2,2′-bithiophen-5-yl) substitution. Thus, the oxidation of **10** occurs at +0.50 V, which is higher than that of **9** by only 30 mV.

Theoretical Calculations. To obtain further insights into the electronic properties, we performed the time-dependent (TD) DFT calculations for **1**–**10**. The results for absorption energies of **1**–**10** at the TD-B3LYP/6-31G*//B3LYP/6-31G* level of theory with the ground-state geometries are summarized in Table 1. The absorption maxima in the low-energy region of **4**, **5**, **9**, and **10** are related to the HOMO–LUMO transitions, whereas those of **1a,b**, **2**, **3**, and **6**–**8** are attributed to the transitions from the HOMO, HOMO-1, and HOMO-2 into the LUMO, LUMO+1, LUMO+2, and LUMO +3 levels. The calculated λ_{max} values are blue-shifted with respect to the experimental values by 14–32 nm except for **5** and **6**, which probably reflects that the calculations were performed under the gas-phase conditions. Compounds **1**–**10** follow the experimentally observed trend for the longest λ_{max}, where the introduction of the thienyl groups at the 2,7-positions than the 1,8- and/or *N*- and 3,6-positions resulted in the more red-shifted absorption bands (*vide supra*). The red shifts of the longest λ_{max} values observed in the electronic absorption spectra upon increasing the number of thiophene units from **3** (345 nm) to **9** (380 nm) and from **4** (370 nm) to **10** (399 nm) are nicely reproduced in the calculations.

The electronic effects of the thienyl groups in the carbazole moiety were studied by molecular orbital calculations. The frontier molecular orbital (FMO) plots and the HOMO and LUMO levels of **1**–**10** were obtained by the single-point calculations at the B3LYP/6-311G**//B3LYP/6-31G* level of theory. The results are summarized in Table 2, and the HOMOs and LUMOs of **1**–**5** and **6**–**10** are shown in Figures 4 and 5, respectively. The calculated HOMO–LUMO gaps are higher than those obtained from the UV–vis absorption spectra by *ca.* 1 eV, which probably reflects that the optical gaps are estimated under the solution conditions, whereas the theoretical gaps are estimated under the gas-phase conditions as described above. However, it is noted that the calculations qualitatively reproduce the findings that the 2,2′-bithiophen-5-yl substitution generally resulted in the decrease of the HOMO–LUMO gaps and the increase of the donor ability as observed in the absorption spectra and the CV, respectively. The

dx.doi.org/10.1021/jo202625p | J. Org. Chem. 2012, 77, 3222–3232

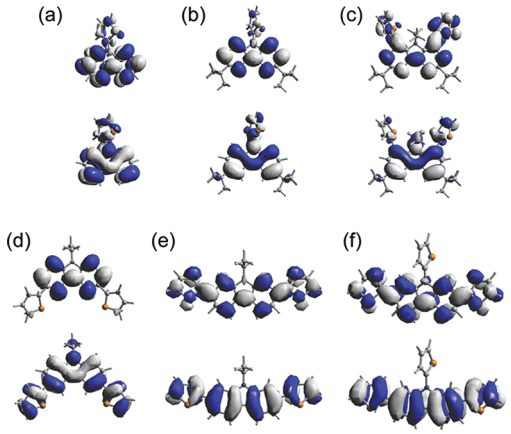

Figure 4. Molecular orbital plots (B3LYP/6-311G**//B3LYP/6-31G*) of (a) **1a**, (b) **1b**, (c) **2**, (d) **3**, (e) **4**, and (f) **5**. The lower plots represent the HOMOs, and the upper plots represent the LUMOs.

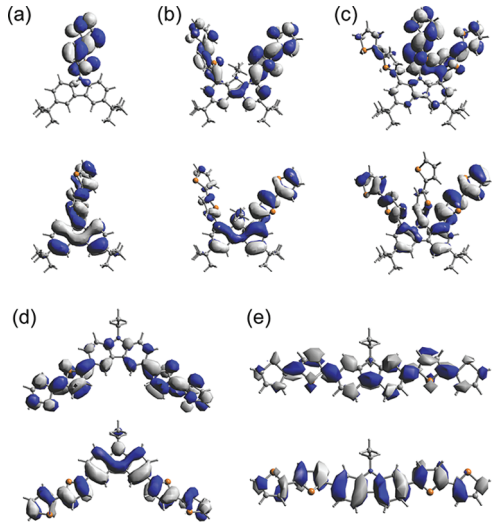

Figure 5. Molecular orbital plots (B3LYP/6-311G**//B3LYP/6-31G*) of (a) **6**, (b) **7**, (c) **8**, (d) **9**, and (e) **10**. The lower plots represent the HOMOs, and the upper plots represent the LUMOs.

calculated HOMO levels of **6**, **7**, **9**, and **10** are higher than those of **1b**, **2**, **3**, and **4**, respectively. Again, the LUMO levels of **6**, **7**, **9**, and **10** are lower than those of **1b**, **2**, **3**, and **4**, respectively. The LUMO levels are more affected than the HOMO levels by the 2,2′-bithiophen-5-yl substitution. Consequently, the calculated gaps of **6**, **7**, **9**, and **10** are smaller than those of **1b**, **2**, **3**, and **4**, respectively. Both the calculated HOMO and LUMO levels of **5** are lower than those of **4**, and no significant difference in their $\Delta E_{\mathrm{HOMO-LUMO}}$ values is observed. This also agrees well with the results in the absorption spectra and the CV.

All HOMO densities are found in the electron-donating carbazole moiety as expected. Almost no π-conjugation between the carbazole and thienyl moieties in **1a,b** is observable in the FMOs as well as the UV−vis spectra and CV (*vide supra*), which may explain the fact that the electron-donating ability of **1a** and **1b** is not enhanced as compared to **23** and **24**, respectively.[37] The HOMO of **2** is also localized in the carbazole moiety, while the HOMOs of **3** and **4** are delocalized over the whole π-skeleton, which results in the destabilization of the HOMOs compared to that of **23** as confirmed by the CV. The difference of the E_{pa} values between **3** and **4** is again clearly rationalized by the calculations, where the HOMO density of **3** has a large contribution from the electron-rich nitrogen atom, whereas that of **4** is not found on the nitrogen atom. Both the HOMO and LUMO densities of **5** have almost no contribution from the *N*-(2-thienyl) group. This justifies the nearly identical absorption profiles of **4** and **5** as shown in Figure 2a. Compared to **1a**, **1b**, and **2**, the HOMO densities of **6**−**8** are more delocalized over the carbazole−bithiophene systems by the π-conjugation. This probably shifts their E_{pa} values cathodically compared to **1a**, **1b**, and **2**. The majority of LUMO densities of **6**−**8** resides on the 2,2′-bithiophen-5-yl unit. Therefore, the longest wavelength absorption bands of **6**−**8** may have a somewhat charge-transfer character, which causes the broad emission with large Stokes shifts.[38] The HOMOs and LUMOs of **9** and **10** have an extension of π-conjugation over the whole conjugated backbone.

CONCLUSION

In conclusion, we have synthesized a series of thienylcarbazoles **1**−**10** by Suzuki−Miyaura and Ullmann coupling reactions. The electronic structure was approached by UV−vis and fluorescence spectral measurements, CV, and DFT calculations. We have demonstrated that the substitution pattern of a carbazole moiety and the number of thiophene units play an important role in the electronic structure. The thienyl substituents at the 2,7-positions in **4**, **5**, and **10** cause a high degree of π-conjugation and high fluorescence quantum yields, while those at the 3,6-positions increase the donor ability as demonstrated by the CV for **3** and **9**. Compound **10** also possesses the high donor ability presumably due to the 2,2′-bithiophen-5-yl group. The introduction of the 2,2′-bithiophen-5-yl group in **9** and **10** was found to ensure the extension of π-conjugation compared to **3** and **4**, respectively. It has to be mentioned that the number of thiophene units sufficiently affects the extent of π-conjugation in nonplanar *N*- and/or 1,8-substituted carbazole derivatives: there is almost no π-conjugation between the carbazole and thiophene units in **1a**, **1b**, and **2**, whereas the carbazole and thiophene units in **6**−**8** are substantially π-conjugated. The experimental observations as above are in qualitative agreement with the results obtained by the DFT calculations. Further studies addressing the synthesis and the characteristics of the π-conjugation, emission, and donor ability of new carbazole−thiophene systems are currently underway in our laboratory. We believe that the present study provides valuable information for the synthesis of new carbazole-based π-systems.

EXPERIMENTAL SECTION

General Suzuki−Miyaura Cross-Coupling Procedure for Preparation of Thienylcarbazoles. A mixture of haloarene (1 equiv) and Na_2CO_3 (2.6 equiv) in DME/water (7:1, ∼0.5 M) was bubbled with argon with stirring for 15 min. $Pd(PPh_3)_4$ (0.02 equiv) and boronic acid pinacol ester (1.2 equiv) were added to the mixture, and the resulting mixture was refluxed for 4−20 h under argon atmosphere. After addition of 5% aqueous NH_4Cl to the mixture, the organic phase was separated, and the aqueous phase was extracted with $CHCl_3$. The combined organic phase was washed with brine, dried over anhydrous $MgSO_4$, and evaporated in vacuo. The residue was purified by column chromatography. An analytically pure material was obtained by recycling gel permeation chromatography.

3,6-Di-*tert*-butyl-1,8-di(2-thienyl)-9-ethyl-9*H*-carbazole (2). Compound **11** (0.20 g, 0.43 mmol) was allowed to react with 2-thiopheneboronic acid pinacol ester **12** (0.23 g, 1.07 mmol) for 12 h

dx.doi.org/10.1021/jo202625p | J. Org. Chem. 2012, 77, 3222−3232

according to the general Suzuki–Miyaura cross-coupling procedure. The crude material was purified by column chromatography (SiO_2; hexane/toluene 9:1) to give **2** (64 mg, 32%) as a white solid. Mp 261–263 °C; ^{1}H NMR (300 MHz, $CDCl_3$) δ 0.47 (t, J = 6.9 Hz, 3H), 1.46 (s, 18H), 3.66 (q, J = 6.9 Hz, 2H), 7.10 (dd, J = 3.6, 5.1 Hz, 2H), 7.17 (dd, J = 1.2, 3.6 Hz, 2H), 7.36 (dd, J = 1.2, 5.1 Hz, 2H), 7.40 (d, J = 2.1 Hz, 2H), 8.08 (d, J = 2.1 Hz, 2H); ^{13}C NMR (125 MHz, $CDCl_3$) δ 14.31, 32.06, 34.70, 40.19, 116.37, 118.81, 125.45, 126.17, 127.04, 127.06, 127.87, 139.15, 142.09, 142.73; UV–vis (CH_2Cl_2) λ_{max} (relative intensity) 290 (sh, 0.91), 303 (1.00), 345 (sh, 0.22), 359 (0.23) nm; HR-FAB-MS (NBA, positive) m/z calcd for $C_{30}H_{33}NS_2^+$ 471.2054, found 471.2059 (M^+).

9-Ethyl-2,7-di(2-thienyl)-9*H*-carbazole (4). Compound **13** (0.30 g, 0.85 mmol) was allowed to react with 2-thiopheneboronic acid pinacol ester **12** (0.45 g, 2.12 mmol) for 20 h according to the general Suzuki–Miyaura cross-coupling procedure. The crude material was purified by column chromatography (SiO_2; hexane/toluene 4:1) to give **4** (0.21 g, 68%) as a white solid. Mp 196–198 °C; ^{1}H NMR (300 MHz, $CDCl_3$) δ 1.50 (t, J = 7.2 Hz, 3H), 4.43 (q, J = 7.2 Hz, 2H), 7.13 (dd, J = 3.6, 5.1 Hz, 2H), 7.31 (dd, J = 1.2, 5.1 Hz, 2H), 7.42 (dd, J = 1.2, 3.6 Hz, 2H), 7.51 (dd, J = 1.5, 8.1 Hz, 2H), 7.59 (d, J = 1.5 Hz, 2H), 8.04 (d, J = 8.1 Hz, 2H); ^{13}C NMR (125 MHz, $CDCl_3$) δ 14.04, 37.70, 105.88, 118.00, 120.87, 122.39, 123.24, 124.77, 128.23, 132.31, 141.04, 145.68; UV–vis (CH_2Cl_2) λ_{max} (relative intensity) 269 (0.92), 290 (sh, 0.36), 353 (1.00), 370 (sh, 0.81) nm; HR-FAB-MS (NBA, positive) m/z calcd for $C_{22}H_{17}NS_2^+$ 359.0802, found 359.0795 (M^+).

2,7,9-Tri(2-thienyl)-9*H*-carbazole (5). Compound **16** (0.15 g, 0.36 mmol) was allowed to react with 2-thiopheneboronic acid pinacol ester **12** (0.19 g, 0.92 mmol) for 4 h according to the general Suzuki–Miyaura cross-coupling procedure. The crude material was purified by column chromatography (SiO_2; hexane/CH_2Cl_2 10:1) to give **5** (140 mg, 92%) as a pale yellow solid. Mp 203–204 °C; ^{1}H NMR (300 MHz, $CDCl_3$) δ 7.08 (dd, J = 3.6, 5.1 Hz, 2H), 7.22 (dd, J = 1.6, 3.8 Hz, 1H). 7.24–7.26 (m, 1H), 7.27 (dd, J = 1.2, 5.1 Hz, 2H), 7.35 (dd, J = 1.2, 3.6 Hz, 2H), 7.44 (dd, J = 1.6, 5.4 Hz, 1H), 7.57 (dd, J = 1.2, 8.1 Hz, 2H), 7.62 (d, J = 1.2 Hz, 2H), 8.04 (d, J = 8.1 Hz, 2H); ^{13}C NMR (125 MHz, $CDCl_3$) δ 107.48, 119.61, 120.69, 122.78, 123.45, 124.82, 124.95, 125.32, 126.56, 128.18, 132.95, 138.22, 143.14, 145.15; UV–vis (CH_2Cl_2) λ_{max} (relative intensity) 261 (0.76), 292 (0.33), 352 (1.00) nm; HR-FAB-MS (NBA, positive) m/z calcd for $C_{24}H_{15}NS_3^+$ 413.0367, found 413.0356 (M^+).

1,8-Bis(2,2′-bithiophen-5-yl)-3,6-di-*tert*-butyl-9-ethyl-9*H*-ethylcarbazole (7). Compound **20** (64 mg, 0.11 mmol) was allowed to react with 2,2′-bithiophene-5-boronic acid pinacol ester **14** (100 mg, 0.34 mmol) for 4 h according to the general Suzuki–Miyaura cross-coupling procedure. The crude material was purified by column chromatography (SiO_2; hexane/toluene 10:1) to give **7** (46 mg, 63%) as a pale yellow solid. Mp 220–222 °C; ^{1}H NMR (300 MHz, $CDCl_3$) δ 0.53 (t, J = 6.9 Hz, 3H), 1.47 (s, 18H), 3.94 (q, J = 6.9 Hz, 2H), 7.03 (dd, J = 3.6, 5.1 Hz, 2H), 7.10 (d, J = 3.6 Hz, 2H), 7.19 (d, J = 3.6 Hz, 2H), 7.20–7.24 (m, 4H), 7.44 (d, J = 1.8 Hz, 2H), 8.08 (d, J = 1.8 Hz, 2H); ^{13}C NMR (125 MHz, $CDCl_3$) δ 14.20, 32.05, 32.15, 34.74, 116.56, 118.69, 123.73, 124.43, 125.19, 126.54, 127.60, 127.75, 127.98, 137.36, 137.54, 139.32, 140.96, 143.11; UV–vis (CH_2Cl_2) λ_{max} (relative intensity) 310 (1.00), 325 (sh, 0.92), 370 (0.52) nm; HR-FAB-MS (NBA, positive) m/z calcd for $C_{38}H_{37}NS_4^+$ 635.1809, found 635.1805 (M^+).

3,6-Bis(2,2′-bithiophen-5-yl)-9-ethyl-9*H*-carbazole (9). Compound **22** (0.08 g, 0.23 mmol) was allowed to react with 2,2′-bithiophene-5-boronic acid pinacol ester **14** (0.20 g, 0.68 mmol) for 17 h according to the general Suzuki–Miyaura cross-coupling procedure. The crude material was purified by column chromatography (SiO_2; hexane/CH_2Cl_2 10:1) to give **9** (102 mg, 85%) as a yellow solid. Mp 171–174 °C; ^{1}H NMR (300 MHz, $CDCl_3$) δ 1.47 (t, J = 6.9 Hz, 3H), 4.39 (q, J = 6.9 Hz, 2H), 7.05 (dd, J = 3.6, 5.0 Hz, 2H), 7.19 (d, J = 3.6 Hz, 2H), 7.21 (d, J = 5.0 Hz, 2H), 7.22 (d, J = 3.6 Hz, 2H), 7.28 (d, J = 3.6 Hz, 2H), 7.41 (d, J = 8.4 Hz, 2H), 7.75 (dd, J = 1.8, 8.4 Hz, 2H), 8.35 (d, J = 1.8 Hz, 2H); ^{13}C NMR (125 MHz, $CDCl_3$) δ 14.05, 37.94, 109.17, 117.85, 122.77, 123.38, 123.42, 124.15, 124.38, 124.81, 125.73, 127.99, 135.62, 137.89, 140.06, 144.54; UV–vis (CH_2Cl_2) λ_{max} (relative intensity) 353 (1.00), 380 (0.97) nm; HR-FAB-MS (NBA, positive) m/z calcd for $C_{30}H_{21}NS_4^+$ 523.0557, found 523.0593 (M^+).

2,7-Bis(2,2′-bithiophen-5-yl)-9-ethyl-9*H*-carbazole (10). Compound **13** (80 mg, 0.22 mmol) was allowed to react with 2,2′-bithiophene-5-boronic acid pinacol ester **14** (0.14 g, 0.68 mmol) for 17 h according to the general Suzuki–Miyaura cross-coupling procedure. The crude material was purified by column chromatography (SiO_2; hexane/toluene 4:1 to toluene) to give **10** (97 mg, 81%) as a yellow solid. Mp 255–256 °C; ^{1}H NMR (300 MHz, $CDCl_3$) δ 1.53 (t, J = 7.3 Hz, 3H), 4.45 (q, J = 7.3 Hz, 2H), 7.05 (dd, J = 3.6, 4.4 Hz, 2H), 7.20 (d, J = 3.6 Hz, 2H), 7.23 (d, J = 3.6 Hz, 2H), 7.23 (d, J = 4.4 Hz, 2H), 7.34 (d, J = 3.6 Hz, 2H), 7.51 (dd, J = 1.4, 8.1 Hz, 2H), 7.58 (d, J = 1.4 Hz, 2H), 8.05 (d, J = 8.1 Hz, 2H); ^{13}C NMR (125 MHz, $CDCl_3$): not available due to the low solubility; UV–vis (CH_2Cl_2) λ_{max} (relative intensity) 256 (0.56), 313 (0.20), 399 (1.00) nm; HR-FAB-MS (NBA, positive) m/z calcd for $C_{30}H_{21}NS_4^+$ 523.0557, found 523.0565 (M^+).

1,8-Bis(2,2′-bithiophen-5-yl)-3,6-di-*tert*-butyl-9*H*-carbazole (21). Compound **19** (0.23 g, 0.43 mmol) was allowed to react with 2,2′-bithiophene-5-boronic acid pinacol ester **14** (0.38 g, 1.30 mmol) for 6 h according to the general Suzuki–Miyaura cross-coupling procedure. The crude material was purified by column chromatography (SiO_2; hexane/toluene 4:1) to give **21** (0.12 g, 60%) as a yellow solid. Mp 220–223 °C; ^{1}H NMR (300 MHz, $CDCl_3$) δ 1.50 (s, 18H), 7.05 (dd, J = 3.9, 5.4 Hz, 2H), 7.24–7.26 (m, 4H), 7.28 (d, J = 3.6 Hz, 2H), 7.36 (d, J = 3.6 Hz, 2H), 7.65 (d, J = 2.1 Hz, 2H), 8.08 (d, J = 2.1 Hz, 2H), 8.90 (s, 1H); ^{13}C NMR (125 MHz, $CDCl_3$) δ 32.16, 34.96, 116.57, 117.26, 123.22, 123.98, 124.54, 124.71, 124.76, 125.19, 128.06, 135.32, 136.87, 137.31, 140.57, 143.45; UV–vis (CH_2Cl_2) λ_{max} (relative intensity) 325 (1.00), 379 (0.69) nm; HR-FAB-MS (NBA, positive) m/z calcd for $C_{36}H_{33}NS_4^+$ 607.1496, found 607.1479 (M^+).

General Ullmann Coupling Procedure for Preparation of Thienylcarbazoles. A mixture of carbazole derivative (1 equiv), bromoarene (1.2 equiv), K_2CO_3 (3 equiv), and copper powder (3 equiv) in nitrobenzene (~0.5 M) was stirred at 180 °C for 24 h. After the precipitate was removed by filtration, the filtrate was concentrated in vacuo. The residue was purified by column chromatography. An analytically pure sample was obtained by recycling gel permeation chromatography.

9-(2,2′-Bithiophen-5-yl)-3,6-di-*tert*-butyl-9*H*-carbazole (6). Compound **17** (0.28 g, 1.00 mmol) was allowed to react with **18** (0.29 g, 1.20 mmol) according to the general Ullmann coupling procedure. The crude material was purified by column chromatography (SiO_2; hexane/toluene 4:1) to give **6** (89 mg, 20%) as a yellow solid. Mp 189–191 °C; ^{1}H NMR (300 MHz, $CDCl_3$) δ 1.46 (s, 18H), 7.07 (dd, J = 3.6, 5.1 Hz, 1H), 7.08 (d, J = 3.6 Hz, 1H), 7.20 (d, J = 3.6 Hz, 1H), 7.21 (dd, J = 3.6, 5.1 Hz, 1H), 7.26 (dd, J = 3.6, 5.1 Hz, 1H), 7.45 (d, J = 8.7 Hz, 2H), 7.50 (dd, J = 1.5, 8.7 Hz, 2H), 8.09 (d, J = 1.5 Hz, 2H); ^{13}C NMR (125 MHz, $CDCl_3$) δ 32.12, 34.91, 109.78, 116.37, 122.43, 123.65, 123.99, 124.07, 124.83, 124.91, 128.05, 135.31, 137.32, 138.00, 140.25, 143.81; UV–vis (CH_2Cl_2) λ_{max} (relative intensity) 260 (sh, 0.76), 285 (sh, 0.75), 296 (1.00), 325 (sh, 0.66), 340 (0.74) nm; HR-FAB-MS (NBA, positive) m/z calcd for $C_{28}H_{29}NS_2^+$ 443.1741, found 443.1743 (M^+).

3,6-Di-*tert*-butyl-1,8,9-tris(2,2′-bithiophen-5-yl)-9*H*-carbazole (8). Compound **21** (80 mg, 0.13 mmol) was allowed to react with **18** (39 mg, 0.15 mmol) according to the general Ullmann coupling procedure. The crude material was purified by column chromatography (SiO_2; hexane/toluene 3:1) to give **8** (65 mg, 65%) as a yellow solid. Mp 213-214 °C; ^{1}H NMR (300 MHz, $CDCl_3$) δ 1.49 (s, 18H), 6.35 (d, J = 3.9 Hz, 1H), 6.40 (d, J = 3.9 Hz, 1H), 6.48 (d, J = 3.6 Hz, 2H), 6.74 (d, J = 3.6 Hz, 2H), 6.79 (dd, J = 0.9, 3.3 Hz, 1H), 6.86 (dd, J = 3.6, 5.1 Hz, 1H), 6.95 (dd, J = 3.6, 5.1 Hz, 2H), 7.00 (dd, J = 0.9, 3.6 Hz, 2H), 7.11 (dd, J = 0.9, 3.6 Hz, 1H), 7.15 (dd, J = 0.9, 5.1 Hz, 2H), 7.45 (d, J = 2.1 Hz, 2H), 8.15 (d, J = 2.1 Hz, 2H); ^{13}C NMR (125 MHz, $CDCl_3$) δ 32.03, 34.81, 116.65, 118.67, 121.36, 123.42, 123.53, 123.94, 124.19, 124.60, 124.89, 127.66, 127.78, 128.65, 128.77, 128.94, 136.19, 137.00, 137.31, 137.59, 139.28, 139.52, 143.63 (1 peak was missing); UV–vis (CH_2Cl_2) λ_{max} (relative intensity) 305

(1.00), 335 (sh, 0.70) nm; HR-FAB-MS (NBA, positive) m/z calcd for $C_{44}H_{37}NS_6^+$ 771.1250, found 771.1315 (M^+).

2,7-Dibromo-9-(2-thienyl)-9*H*-carbazole (16). Compound **15** (400 mg, 1.24 mmol) was allowed to react with 2-bromothiophene (1.2 mL, 12.5 mmol) according to the general Ullmann coupling procedure. The crude material was purified by column chromatography (SiO_2; hexane/toluene 4:1) give **16** (374 mg, 75%) as a yellow solid. Mp 233−235 °C; ^{1}H NMR (300 MHz, $CDCl_3$) δ 7.19−7.22 (m, 2H), 7.41 (dd, J = 1.8, 8.7 Hz, 2H), 7.44 (dd, J = 2.4, 4.8 Hz, 1H), 7.53 (d, J = 1.8 Hz, 2H), 7.90 (d, J = 8.7 Hz, 2H); ^{13}C NMR (125 MHz, $CDCl_3$) δ 113.63, 120.39, 121.52, 121.90, 124.38, 125.42, 125.83, 126.67, 137.14, 143.07; UV−vis (CH_2Cl_2) λ_{max} (relative intensity) 294 (0.71), 303 (1.00), 323 (0.22), 336 (0.14) nm; HR-FAB-MS (NBA, positive) m/z calcd for $C_{16}H_9Br_2NS^+$ 404.8822, found 404.8836 (M^+).

3,6-Di-*tert*-butyl-1,8-diiodo-9-ethyl-9*H*-carbazole (20). A mixture of **19** (50 mg, 0.094 mmol), NaOH (15 mg, 0.37 mmol), and iodoethane (15 μL, 0.19 mmol) in DMF was stirred at 45 °C for 3 h. The mixture was poured into water, and the resulting solution was extracted with toluene/ethyl acetate. The organic layer was dried over anhydrous $MgSO_4$ and evaporated in vacuo. The residue was purified by column chromatography (SiO_2; hexane) to give **20** (50 mg, 95%) as a white solid. Mp 171−172 °C; ^{1}H NMR (300 MHz, $CDCl_3$) δ 1.22 (t, J = 7.2 Hz, 3H), 1.41 (s, 18H), 5.22 (q, J = 7.2 Hz, 2H), 7.97 (d, J = 1.8 Hz, 2H), 7.99 (d, J = 1.8 Hz, 2H); ^{13}C NMR (125 MHz, $CDCl_3$) δ 16.61, 31.89, 34.52, 38.02, 73.55, 116.05, 126.00, 137.87, 139.09, 144.89; UV−vis (CH_2Cl_2) λ_{max} (relative intensity) 254 (1.00), 265 (sh, 0.73), 275 (sh, 0.55), 290 (sh, 0.40), 300 (0.49), 335 (sh, 0.09), 348 (0.13), 362 (0.12) nm; HR-FAB-MS (NBA, positive) m/z calcd for $C_{22}H_{27}I_2N^+$ 559.0233, found 559.0146 (M^+).

■ ASSOCIATED CONTENT

Ⓢ Supporting Information

General experimental methods, X-ray data, UV−vis data, Cartesian coordinates of all calculated molecules, and ^{1}H and ^{13}C NMR spectra of all new compounds. This material is available free of charge via the Internet at http://pubs.acs.org.

■ AUTHOR INFORMATION

Corresponding Author

*E-mail: nakamura@gunma-u.ac.jp. Tel: +81 277 30 1310. Fax: +81 277 30 1314.

Notes

The authors declare no competing financial interest.

■ ACKNOWLEDGMENTS

We thank Prof. Dr. Soichiro Kyushin (Gunma University) for generous permission to use an X-ray diffractometer and Prof. Dr. Teruo Shinmyozu (Kyushu University) for mass spectrometry measurements. This work was performed under the Cooperative Research Program of "Network Joint Research Center for Materials and Devices" (Kyushu University).

■ REFERENCES

(1) (a) Special issue on organic electronics: *J. Mater. Res.* **2004**, *19*, 1887−2203; Faupel, F., Dimitrakopoulos, C., Kahn, A., Wöll, C., Eds. (b) *Organic Electronics: Materials, Manufacturing and Applications*; Klauk, H., Ed.; Wiley-VCH: Weinheim, 2006. (c) Special issue on organic electronics and opto-electronics: *Chem. Rev.* **2007**, *107*, 923−1386; Forrest, S. R., Thompson, M. E., Eds.

(2) (a) *Organic Light Emitting Devices: Synthesis, Properties and Applications*; Müllen, K., Scherf, U., Eds.; Wiley-VCH: Weinheim, 2006. (b) *Organic Electroluminescence*; Kakafi, Z. H., Ed.; CRC Press: New York, 2005.

(3) (a) Dimitrakopoulos, C. D.; Malenfant, P. R. L. *Adv. Mater.* **2002**, *14*, 99−117. (b) Newman, C. R.; Frisbie, C. D.; da Silva Filho, D. A.; Brédas, J.-L.; Ewbank, P. C.; Mann, K. R. *Chem. Mater.* **2004**, *16*, 4436−4451. (c) Murphy, A. R.; Fréchet, J. M. *Chem. Rev.* **2007**, *107*, 1066−1096. (d) Anthony, J. E. *Angew. Chem., Int. Ed.* **2008**, *47*, 452−483. (e) Mas-Torrent, M.; Rovira, C. *Chem. Soc. Rev.* **2008**, *37*, 827−838. (f) Yamashita, Y. *Sci. Technol. Adv. Mater.* **2009**, *10*, 024313.

(4) (a) *Organic Photovoltaics*; Brabec, C., Cyakonov, V., Scherf, U., Eds.; Wiley-VCH: Weinheim, 2008. (b) Thompson, B. C.; Fréchet, J. M. *Angew. Chem., Int. Ed.* **2008**, *47*, 58−77. (c) Cheng, Y.-J.; Yang, S.-H.; Hsu, C.-S. *Chem. Rev.* **2009**, *109*, 5868−5923.

(5) (a) Chen, J.; Reed, M. A.; Dirk, S. M.; Price, D. W.; Rawlett, A. M.; Tour, J. M.; Grubisha, D. S.; Bennet, D. W. In *Molecular Electronics: Bio-Sensors and Bio-Computers*; NATO Science Series II: Mathematics, Physics, Chemistry; Plenum: New York, 2003; Vol. *96*, pp 59−195. (b) Thomas, S. W. III; Joly, G. D.; Swager, T. M. *Chem. Rev.* **2007**, *107*, 1339−1386.

(6) (a) *Electronic Materials: The Oligomer Approach*; Müllen, K., Wegner, G., Eds., Wiley-VCH; Weinheim, 1998. (b) Martin, R. E.; Diederich, F. *Angew. Chem., Int. Ed.* **1999**, *38*, 1350−1377. (c) Segura, J. L.; Martín, N. *J. Mater. Chem.* **2000**, *10*, 2403−2435.

(7) For recent reviews, see: (a) Grazulevicius, J. V.; Strohriegl, P.; Pielichowski, J.; Pielichowski, K. *Prog. Polym. Sci.* **2003**, *28*, 1297−1353. (b) Morin, J.-F.; Leclerc, M.; Adès, D.; Siove, A. *Macromol. Rapid Commun.* **2005**, *26*, 761−778. (c) Blouin, N.; Leclerc, M. *Acc. Chem. Res.* **2008**, *41*, 1110−1119. (d) Boudreault, P.-L. T.; Morin, J.-F.; Leclerc, M. In *Design and Synthesis of Conjugated Polymers*; Leclerc, M., Morin, J.-F., Eds.; Wiley-VCH: Weinheim, 2010; pp 205−226.

(8) For selected examples of light-emitting materials, see: (a) Morin, J.-F.; Bourdreault, P.; Leclerc, M. *Macromol. Rapid Commun.* **2002**, *23*, 1032−1036. (b) Liu, Y.; Nishiura, M.; Wang, Y.; Hou, Z. *J. Am. Chem. Soc.* **2006**, *128*, 5592−5593. (c) Adhikari, R. M.; Mondal, R.; Shah, B. K.; Neckers, D. C. *J. Org. Chem.* **2007**, *72*, 4727−4732. (d) Zhao, Z.; Zhao, Y.; Lu, P.; Tian, W. *J. Phys. Chem. C* **2007**, *111*, 6883−6888. (e) Zhao, Z.; Xu, X.; Wang, H.; Lu, P.; Yu, G.; Liu, Y. *J. Org. Chem.* **2008**, *73*, 594−602. (f) Zhao, Z.; Li, J.-H.; Chen, X.; Wang, X.; Lu, P.; Yang, Y. *J. Org. Chem.* **2009**, *74*, 383−395. (g) Wang, H.-Y.; Liu, F.; Xie, L.-H.; Tang, C.; Peng, B.; Huang, W.; Wei, W. *J. Phys. Chem. C* **2011**, *115*, 6961−6967.

(9) For selected examples of host materials for emitters, see: (a) Brunner, K.; van Dijken, A.; Börner, H.; Bastiaansen, J. J. A. M.; Kiggen, N. M. M.; Langeveld, B. M. W. *J. Am. Chem. Soc.* **2004**, *126*, 6035−6042. (b) van Dijken, A.; Bastiaansen, J. J. A. M.; Kiggen, N. M. M.; Langeveld, B. M. W.; Rothe, C.; Monkman, A.; Bach, I.; Stössel, P.; Brunner, K. *J. Am. Chem. Soc.* **2004**, *126*, 7718−7727. (c) Tsai, M.-H.; Lin, H.-W.; Su, H.-C.; Ke, T.-H.; Wu, C.-c.; Fang, F.-C.; Liao, Y.-L.; Wong, K.-T.; Wu, C.-I. *Adv. Mater.* **2006**, *18*, 1216−1220. (d) Tao, Y.; Wang, Q.; Yang, C.; Wang, Q.; Zhang, Z.; Zou, T.; Qin, J.; Ma, D. *Angew. Chem., Int. Ed.* **2008**, *47*, 8104−8107. (e) Kim, S. H.; Cho, I.; Sim, M. K.; Park, S.; Park, S. Y. *J. Mater. Chem.* **2011**, *21*, 9139−9148. (f) Chen, Y.-M.; Hung, W.-Y.; You, H.-W.; Chaskar, A.; Ting, H.-C.; Chen, H.-F.; Wong, K.-T.; Liu, Y.-H. *J. Mater. Chem.* **2011**, *21*, 14971−14978.

(10) (a) Drolet, N.; Morin, J.-F.; Leclerc, N.; Wakim, S.; Tao, Y.; Leclerc, M. *Adv. Funct. Mater.* **2005**, *15*, 1671−1682. (b) Sonntag, M.; Kreger, K.; Hanft, D.; Strohriegl, P. *Chem. Mater.* **2005**, *17*, 3031−3039. (c) Wakim, S.; Blounin, N.; Gingras, E.; Tao, Y.; Leclerc, M. *Macromol. Rapid Commun.* **2007**, *28*, 1798−1803. (d) Song, Y.; Di, C.-a.; Wei, Z.; Zhao, T.; Xu, W.; Liu, Y.; Zhang, D.; Zhu, D. *Chem.—Eur. J.* **2008**, *14*, 4731−4740. (e) Li, Z.; Liu, Y.; Yu, G.; Wen, Y.; Guo, Y.; Ji, L.; Qin, J.; Li, Z. *Adv. Funct. Mater.* **2009**, *19*, 2677−2683.

(11) For a review on carbazole derivatives for photovoltaic devices, see: (a) Beaupré, S.; Boudreault, P.-L. T.; Leclerc, M. *Adv. Mater.* **2010**, *22*, E6−E27. See also: (b) Blounin, N.; Michaud, D.; Gendron, D.; Wakim, S.; Blair, E.; Neagu-Plesu, R.; Belletête, M.; Durocher, G.; Tao, Y.; Leclerc, M. *J. Am. Chem. Soc.* **2008**, *130*, 732−742. (c) Blounin, N.; Michaud, A.; Leclerc, M. *Adv. Mater.* **2007**, *19*, 2295−2300. (d) Peng, B.; Najari, A.; Liu, B.; Berrouard, P.; Gendron, D.; He, Y.; Zhou, K.; Leclerc, M.; Zou, Y. *Macromol. Chem. Phys.* **2010**, *211*, 2026−2033.

(12) (a) Moser, M.; Wucher, B.; Kunz, D.; Rominger, F. *Organometallics* **2007**, *26*, 1024−1030. (b) Mudadu, M. S.; Singh, A.

N.; Thummel, R. P. *J. Org. Chem.* **2008**, *73*, 6513−6520. (c) Barbe, J.-M.; Habermeyer, B.; Khoury, T.; Gros, C. P.; Richard, P.; Chen, P.; Kadish, K. M. *Inorg. Chem.* **2010**, *49*, 8929−8940.
(13) (a) Hassan, L. A.; Norouzi-Arasi, H.; Wagner, M.; Enkelmann, V.; Müllen, K. *Chem. Commun.* **2011**, *47*, 970−972. (b) Maeda, C.; Yoneda, T.; Aratani, N.; Yoon, M.-C.; Lim, J. M.; Kim, D.; Yoshioka, N.; Osuka, A. *Angew. Chem., Int. Ed.* **2011**, *50*, 5691−5694.
(14) (a) Michinobu, T.; Osako, H.; Shigehara, K. *Macromol. Rapid Commun.* **2008**, *29*, 111−116. (b) Michinobu, T.; Osako, H.; Shigehara, K. *Macromolecules* **2009**, *42*, 8172−8180. (c) Michinobu, T.; Osako, H.; Murata, K.; Shigehara, K. *Chem. Lett.* **2010**, *39*, 168−169.
(15) (a) Mishra, A.; Ma, C.-Q.; Bäuerle, P. *Chem. Rev.* **2009**, *109*, 1141−1276. (b) *Handbook of Thiophene-based Materials*; Perepichka, I. F., Perepichka, D. F., Eds.; Wiley-VCH: Weinheim, 2009.
(16) Zhan, X.; Liu, Y.; Zhu, D.; Jiang, X.; Jen, A. K.-Y. *Macromol. Chem. Phys.* **2001**, *202*, 2341−2345.
(17) Zotti, G.; Schiavon, G.; Zecchin, S.; Morin, J.-F.; Leclerc, M. *Macromolecules* **2002**, *35*, 2122−2128.
(18) Melucci, M.; Favaretto, L.; Bettini, C.; Gazzano, M.; Camaioni, N.; Maccagnani, P.; Ostoja, P.; Monari, M.; Barbarella, G. *Chem.—Eur. J.* **2007**, *13*, 10046−10054.
(19) (a) Morin, J.-F.; Drolet, N.; Tao, Y.; Leclerc, M. *Chem. Mater.* **2004**, *16*, 4619−4626. (b) Belletête, M.; Bouchard, J.; Leclerc, M.; Durocher, G. *Macromolecules* **2005**, *38*, 880−887. (c) Lu, J.; Xia, P. F.; Lo, P. K.; Tao, Y.; Wong, M. S. *Chem. Mater.* **2006**, *18*, 6194−6203. (d) Promark, V.; Pankvuang, A.; Ruchirawat, S. *Tetrahedron Lett.* **2007**, *48*, 1151−1154. (e) Promarak, V.; Ruchirawat, S. *Tetrahedron* **2007**, *63*, 1602−1609. (f) Promarak, V.; Punkvuang, A.; Sudyoadsuk, T.; Jungsuttiwong, S.; Saengsuwan, S.; Keawin, T.; Sirithip, K. *Tetrahedron* **2007**, *63*, 8881−8890.
(20) (a) Belltête, M.; Bédard, M.; Leclerc, M.; Durocher, G. *Synth. Met.* **2004**, *146*, 99−108. (b) Yang, Li.; Feng, J.-K.; Ren, A.-M.; Sun, J.-Z. *Polymer* **2006**, *47*, 1397−1404. (c) Doskocz, J.; Doskocz, M.; Roszak, S.; Soloducho, J.; Leszczynski, J. *J. Phys. Chem. A* **2006**, *110*, 13989−13994.
(21) For a preliminary communication of this work, see: Shimizu, H.; Kobayashi, A.; Itoi, S.; Yoshihara, T.; Tobita, S.; Nakamura, Y.; Nishimura, J. *Heterocycles* **2009**, *78*, 1265−1269.
(22) Wu, I.-Y.; Lin, J. T.; Tao, Y.-T.; Balasubramaniam, E.; Su, Y. Z.; Ko, C.-W. *Chem. Mater.* **2001**, *13*, 2626−2631.
(23) Hameurlaine, A.; Dehaen, W. *Tetrahedron Lett.* **2003**, *44*, 957−959.
(24) Park, M.; Buck, J. R.; Rizzo, C. J. *Tetrahedron* **1998**, *54*, 12707−12714.
(25) Miyaura, N.; Suzuki, A. *Chem. Rev.* **1995**, *95*, 2457−2483.
(26) Hassan, J.; Sevignon, M.; Gozzi, C.; Schulz, E.; Lemaire, M. *Chem. Rev.* **2002**, *102*, 1359−1469.
(27) For the crystal packing structures of **5** and **9**, see the Supporting Information.
(28) Frisch, M. J.; Trucks, G. W.; Schlegel, H. B.; Scuseria, G. E.; Robb, M. A.; Cheeseman, J. R.; Montgomery, J. A., Jr.; Vreven, T.; Kudin, K. N.; Burant, J. C.; Millam, J. M.; Iyengar, S. S.; Tomasi, J.; Barone, V.; Mennucci, B.; Cossi, M.; Scalmani, G.; Rega, N.; Petersson, G. A.; Nakatsuji, H.; Hada, M.; Ehara, M.; Toyota, K.; Fukuda, R.; Hasegawa, J.; Ishida, M.; Nakajima, T.; Honda, Y.; Kitao, O.; Nakai, H.; Klene, M.; Li, X.; Knox, J. E.; Hratchian, H. P.; Cross, J. B.; Bakken, V.; Adamo, C.; Jaramillo, J.; Gomperts, R.; Stratmann, R. E.; Yazyev, O.; Austin, A. J.; Cammi, R.; Pomelli, C.; Ochterski, J. W.; Ayala, P. Y.; Morokuma, K.; Voth, G. A.; Salvador, P.; Dannenberg, J. J.; Zakrzewski, V. G.; Dapprich, S.; Daniels, A. D.; Strain, M. C.; Farkas, O.; Malick, D. K.; Rabuck, A. D.; Raghavachari, K.; Foresman, J. B.; Ortiz, J. V.; Cui, Q.; Baboul, A. G.; Clifford, S.; Cioslowski, J.; Stefanov, B. B.; Liu, G.; Liashenko, A.; Piskorz, P.; Komaromi, I.; Martin, R. L.; Fox, D. J.; Keith, T.; Al-Laham, M. A.; Peng, C. Y.; Nanayakkara, A.; Challacombe, M.; Gill, P. M. W.; Johnson, B.; Chen, W.; Wong, M. W.; Gonzalez, C.; Pople, J. A. *Gaussian 03*, revision C.02; Gaussian, Inc.: Wallingford, CT, 2004.
(29) We thank referees for checking the optimized structures of **1b** and **2**.
(30) Kato, S.-i.; Noguchi, H.; Kobayashi, A.; Tobita, S.; Nakamura, Y. Unpublished results. The results will be reported elsewhere.
(31) The fluorescence excitation spectra correspond to the absorption spectra.
(32) Ohkita, H.; Ito, S.; Yamamoto, Y.; Tohda, Y.; Tani, K. *J. Phys. Chem. A* **2002**, *106*, 2140−2145.
(33) Poly(2,7-carbazole)s display high fluorescence quantum yields. See ref 7c and 33.
(34) Fu, Y.; Bo, Z. *Macromol. Rapid Commun.* **2005**, *26*, 1704−1710.
(35) Lee, S. A.; Hottta, S.; Nakanishi, F. *J. Phys. Chem. A* **2000**, *104*, 1827−1833.
(36) We assume that the first oxidation potentials of **6**−**10** are ascribed to the carbazole-centered oxidations on the basis of comparison with the oxidation potential of 2,2′-bithiophene (+0.96 V).
(37) It seems that the *N*-(2-thienyl) substituents of **1a** and **1b** slightly contribute to their HOMOs by the σ-π conjugation rather than the π-conjugation.
(38) With decreasing the solvent polarity from CH_2Cl_2 to cyclohexane, the λ_{em} values of **6**−**8** are hypochromically shifted by 4−15 nm.